Yonsei Medical Journal
Vol. 46, No. 1, pp. 95 - 103, 2005

Comparison of Unmonochromatized Synchrotron Radiation and Conventional X-rays in the Imaging of Mammographic Phantom and Human Breast Specimens: A Preliminary Result

Haijo Jung[1,2], Hee-Joung Kim[1,2,3], Eun-Kyung Kim[1,2], Jin-O Hong[2,3], Jung Ho Je[4], Yeukuang Hwu[5], Wen-Li Tsai[5], Giorgio Magaritondo[6], and Hyung-Sik Yoo[1,2]

[1]Department of Diagnostic Radiology, [2]Research Institute of Radiological Science, [3]BK21 Project for Medical Sciences, Yonsei University College of Medicine, Seoul, Korea;
[4]Department of Materials Science and Engineering, Pohang University of Science and Technology, Pohang, Korea;
[5]Institute of Physics, Academia Sinica, Nankang 11529, Taipei;
[6]Taiwan, Institut de physique Appliquee, Ecole Polytechnique Federale de Lausanne, CH-1015 Lausanne, Switzerland.

A simple imaging setup based on the principle of coherence-based contrast X-ray imaging with unmonochromatized synchrotron radiation was used for studying mammographic phantom and human breast specimens. The use of unmonochromatized synchrotron radiation simplifies the instrumentation, decreases the cost and makes the procedure simpler and potentially more suitable for clinical applications. The imaging systems consisted of changeable silicon wafer attenuators, a tungsten slit system, a $CdWO_4$ scintillator screen, a CCD (Charge Coupled Device) camera coupled to optical magnification lenses, and a personal computer. In preliminary studies, a spatial resolution test pattern and glass capillary filled with air bubbles were imaged to evaluate the resOolution characteristics and coherence-based contrast enhancement. Both the spatial resolution and image quality of the proposed system were compared with those of a conventional mammography system in order to establish the characteristic advantages of this approach. The images obtained with the proposed system showed a resolution of at least 25μm on the test pattern with much better contrast, while the images of the capillary filled with air bubbles revealed coherence-based edge enhancement. This result shows that the coherence-based contrast imaging system, which emphasizes the refraction effect from the edge of materials of different refractive indexes, is applicable to imaging studies in fundamental medicine and biology, although further research works will be required before it can be used for clinical applications.

Key Words: Synchrotron radiation, mammography

Received February 11, 2004
Accepted November 9, 2004

This work was jointly supported by the Brain Korea 21 Project for Medical Science, the Research Institute of Radiological Science, Yonsei University, Seoul 120-752, Korea, National Science Council of Taiwan (NSC-89-2112-M-001-044), the POSTECH research fund (1RB9907801), and the Fonds National Suisse de la recherche Scientifique.

Reprint address: requests to Dr. Hee-Joung Kim, Department of Diagnostic Radiology, Yonsei University College of Medicine, 134 Shinchon-dong, Seodaemoon-gu, Seoul 120-752, Korea, Tel: 82-2-361-5753, Fax: 82-2-313-1039, E-mail: hjkim@yumc.yonsei.ac.kr

INTRODUCTION

Conventional X-ray imaging has been used effectively for the early detection of breast cancer, although it lacks the resolution and contrast necessary to detect pre-cancerous microcalcifications and small nodules. Synchrotron radiation (SR), which has recently been introduced as an alternative to conventional X-rays, has properties which allow high resolution imaging down to the micrometer scale. The most crucial property is coherence, which defines the capability of a radiation source to produce detectable wave-like effects, such as diffraction and interference. This has greatly alleviated the problem of insufficient contrast, which is particularly susceptible to occur when high energy X-rays are used for radiological purposes.[1-6]

Several research groups have successfully utilized this new approach based on coherence-based contrast at various synchrotron facilities. Among

the various experimental setups designed to take advantage of coherence-based edge enhancement using monochromatic beam characteristics, such as diffraction enhanced imaging (DEI), interferometry, etc., the approach presented in this paper seems particularly suitable for coherence-based contrast imaging in radiological applications, in which the characteristics of the unmonochromatized beam present certain limitations. The proposed approach uses unmonochromatic synchrotron radiation and has the capability to image boundaries that have small differences in the X-ray refractive index, without the need for sophisticated X-ray optics.[7,8]

At this moment, numerous experimental studies based on our approach have shown high quality characteristics, with results that are either equivalent to or better than those obtained with the other techniques in several respects. For example, it has recently been demonstrated that this approach can perform real time, high resolution coherence-based contrast imaging on live animals.[9,10] The purpose of this paper to establish the desired characteristics and comparative merits of this specific approach based on coherence-based contrast imaging, in order to evaluate its potential uses as a clinical diagnostic and pathological tool.

To evaluate the resolution characteristics and coherence-based edge enhancement achievable by our approach in the context of mammographic imaging, we studied high spatial resolution test patterns, a glass capillary tube filled with air bubbles, and human breast specimens. Herein, we report the preliminary results of these studies, emphasizing the spatial resolution and image quality.

MATERIALS AND METHODS

Synchrotron radiation source and imaging system at PLS 5C1 beamline

The experiment was performed at the 5C1 beamline in the Pohang Light Source (PLS), in Pohang, Korea. The PLS is a third generation SR source consisting of a 2 - 2.5 GeV electron linear accelerator and an electron storage ring supporting beam currents of 400 mA at 2.0 GeV and 250 mA at 2.5 GeV.

The 5C1 bending magnet beamline with a magnetic field of approximately 1 Tesla at PLS was recently constructed for applications using coherence-based contrast X-ray imaging. Following the results of an earlier study, this beamline was constructed so as to specifically use the unmonochromatized synchrotron radiation X-rays (white beam) required for coherence-based contrast imaging. A series of attenuators, each consisting of a silicon wafer with a thickness of 0.6 mm, was placed into the beam, upstream of the sample position, in order to enable the modification of the energy spectra the energy range of 6-25 keV and photon flux of 10^{11} - 10^{12} photons/mm^2/sec, depending on the object being investigated. Simulated energy spectra of the PLS 5C1 white beam with different silicon wafers are depicted in Fig. 1. Basically, using a thicker attenuator allows only the higher energy portion of the SR to pass through the filter and so as to interact with the sample, thus acting as a high pass filter. Therefore, the use of different combinations of attenuators enabled the production of SR with higher average energy and reduced intensity.[11] This imaging system is relatively simple and inexpensive compared to either an X-ray interferometry system or a diffractometry system.[5,12-14] We believe this simplicity and robustness greatly enhances its

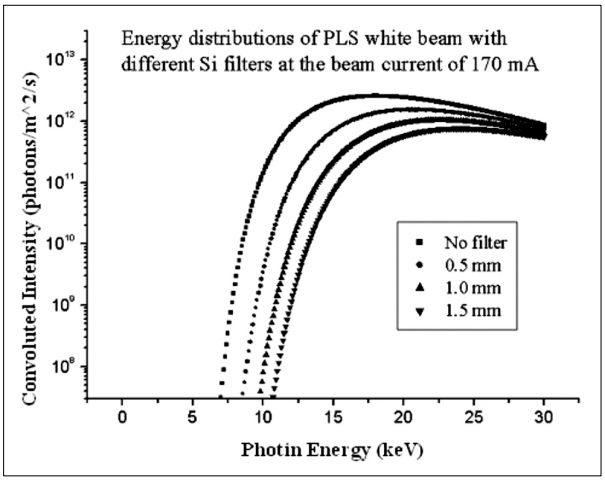

Fig. 1. Energy spectra of PLS white beam for different silicon wafers thicknesses. A series of attenuators was placed in the beam upstream of the sample position and the energy range and the photon flux were adjusted in the range of 6-25 keV and 10^{11} - 10^{12} photons/mm^2/sec, respectively.

applicability.

The cross sectional dimension of the incident beam is determined by a tungsten slit system, measuring 12 × 6 mm in terms of beam area, in order to match the size of the scintillator screen. The synchrotron radiation X-rays passing through the test objects then interact with the scintillator screen, which consists of a thin plate of $CdWO_4$ (10×10×0.1 mm, Saint-Gobain Crystals & Detectors, Newbury, OH, USA, formerly Bicron Co.) before being converted to a visible light image. These optical images were magnified by optical lenses and captured by CCD cameras (for example, a Kodak model ES 4.0/8 bit, mainly used in the early stages of this work) and transferred to a computer for data acquisition and analysis (Fig. 2).

In this particular imaging setup, the spatial resolution is far from the best that is achievable due to the choice of a rather large field of view for the purpose of comparison. In other words, the limitation in this study is primarily due to the low magnification of the imaging system. For example, when using a Kodak ES 4.0/8 bit CCD camera with an image format of 2048 × 2048 pixels to capture an image on the active area of the 15.2 × 15.2 mm^2 CCD chip after 5 × magnification as shown in most of the figures in this paper, the resolution cannot exceed approximately 2μm (roughly a single pixel). On the other hand, we quantitatively obtained a spatial resolution of about 3μm using a $CdWO_4$ scintillator with a thickness of 0.1 mm at 9.3 × optical magnification.[15] Although lenses with much higher magnification could be used, there was no suitable test pattern available which could be used for the purpose of comparison. A 5 × magnification factor was sufficient for most of the studies. With a

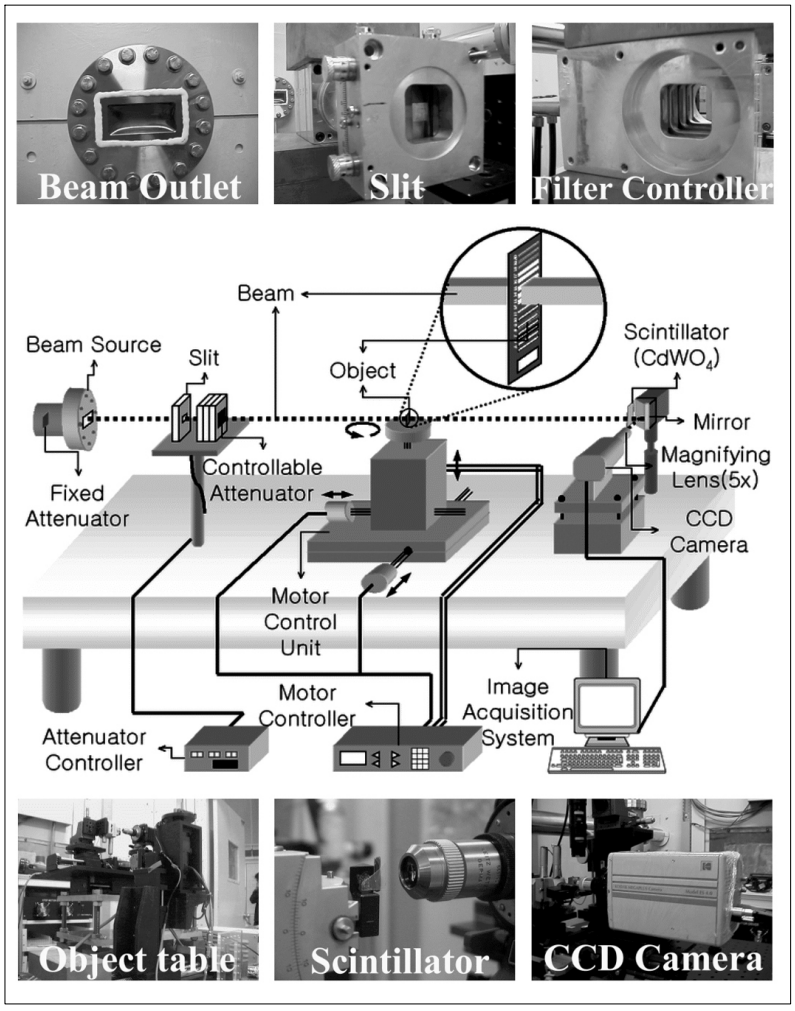

Fig. 2. Schematic diagram of unmonochromatized synchrotron radiation imaging set-up at PLS 5C1 beamline. Synchrotron radiation X-rays passing through the test objects then interact with the scintillator screen before being converted to a visible light image. The optical images were magnified by optical lenses, captured by a CCD camera and transferred to a computer for data acquisition and analysis.

thinner scintillator and larger magnification (smaller field-of-view), we achieved a resolution of better than 1μm. It has also been demonstrated that the resolution in coherence-based radiology is limited by the detector. Using an electron microscope type of imaging system to magnify photoelectrons (received from a photocathode), instead of using an optical lens to received visible photons (scintillator), a resolution of better than 0.3μm can be achieved.[16] Nevertheless, it is not the objective of this paper to demonstrate high resolution, but rather to demonstrate the superior image quality that can be obtained, by using coherence-based edge enhancement, rather than the conventional mammography system.

The sample to scintillator distances were varied from 170 to 470 mm, and the optimal image condition depended on the test objects, since edge enhancement based on the refraction effect strongly depends on the exact three-dimensional structure of the sample. During the measurements, the test objects were scanned by means of a multi-axis mechanical stage and the complete sample image was obtained by patching smaller individual images together.

Spatial resolution and image contrast of PLS 5C1 synchrotron imaging system

The number of attenuators, the distance between the test object and the scintillator screen, and the CCD camera shutter speed were adjusted so as to optimize the high image quality. The resolution test pattern was imaged by placing it directly on the scintillator screen, free from any coherence-based edge enhancement and possible edge blurring, in order to evaluate the spatial resolution characteristics of the PLS 5C1 synchrotron imaging system. The spatial resolution test pattern (Nuclear Associates Co., Hicksville, NY, USA) is made of a gold nickel construction and has a maximum spatial resolution of 20 line-pairs mm-1. The spatial resolution of an imaging system depends on the individual spatial resolution of its components, and the effect this has on the image resolution depends on the type of sample being investigated. The spatial resolutions of the PLS 5C1 SR imaging system were quantitatively measured using an MTF (Modulation Transfer Function) at different optical magnifications and incident beam directions. The MTF was computed from the image of a sharp edge, provided by a thin layer of gold-nickel foil (with a thickness of 0.0175 mm). The electron energy and beam current of the PLS storage during experimentation were approximately 2.5 GeV and 150 mA, respectively. The image acquisition time on the CCD camera (Kodak model ES 4.0/8 bit) ranged from 25 msec to 30 msec. The field of view for the CCD camera (Kodak ES 4.0/8 Bit) with a 5 × magnification lens measured 3.04 × 3.04 mm so that the large final images were obtained by the patching together of multiple smaller images.

For the comparison of the spatial resolution and image contrast between the conventional mammography system (Senographe DMR; GE Medical Systems, Milwaukee, USA) located at Yonsei University Medical Center (YUMC) in Seoul and the synchrotron X-ray imaging system on the PLS 5C1 beamline, the resolution test pattern was directly placed on a screen-film system and imaged with acquisition parameters of 28 kVp, 83 mAs, and Mo/Mo bucky using magnification factors of 1.0 and 1.8. The 1.8 × magnification factor was used to compare the results obtained from the images with the 5C1 synchrotron X-ray imaging system.

To demonstrate the coherence-based edge enhancement provided by the system at object boundaries,[3,8,16,17] a glass capillary tube filled with air bubbles was imaged at varying test object-to-detector distances. The glass tube was prepared by injecting an echocontrast medium granulate, which contains D-galactose and palmitic acid diluted in water (Levovist; Schering AG, Berlin, Germany), into a tube with an outer diameter of 1.6 mm and an inner diameter of 1.1 mm. The images of the glass tube were acquired on a CCD camera (Photometrics CH 250: 1024 × 1024 pixels, 16 depth-bits, active area of 2.52 × 2.52 mm^2) at test object-to-detector (scintillator) distances of 35, 50, 100, 200, 250, 300, 350, and 470 mm. The image acquisition time on the CCD camera was 1,000 msec and the applied thickness of the silicon wafer was 2.5 mm. The field of view of the CCD camera (Photometrics CH 250) coupled with a 5× magnification lens was found to be 5.51 × 5.51 mm^2, as measured using a Veco specimen grid, consisting of a square mesh with a center refer-

ence (Electron Microscope Sciences). During successive image acquisitions, different air bubbles in the glass capillary tube were imaged, because of the thermal expansion of the air bubbles included by the image acquisitions. All of the synchrotron radiation images were background-subtracted to remove the inhomogeneities in the scintillator screen.

Mammographic phantom and cancerous human breast specimen studies

A mammographic accreditation phantom (Gammex RMI 156) was designed to test the performance of the mammographic system by the quantitative evaluation of small structure images that simulate microcalcifications, fibrous structures in ducts, and tumor-like masses in a wax insert. For the comparison of the image quality between the conventional mammography system and the PLS 5C1 synchrotron imaging system, the mammographic accreditation phantom was imaged with both imaging systems. Acquisition parameters of 28 kVp, 79 mAs, and Mo/Mo bucky using a magnification factor of 1.0 were used with the conventional mammography system located at YUMC. Due to the limited field of view of our imaging system, only a small portion of the entire mammographic accreditation phantom was imaged. In particular, those areas containing Al_2O_3 specks simulating microcalcifications were imaged. In this experiment, the object-to-scintillation screen distance was approximately 300 mm.

Ten human breast specimens were prepared with rough dimensions of $10 \times 10 \times 3$ mm^3, as well as rugged surfaces from the biopsy of one patient with a cancerous breast which was preserved in formalin. First, the human breast specimens were imaged with the conventional mammography system at YUMC using acquisition parameters of 22 kVp, 16 mAs, and Mo/Mo bucky using magnification factors of 1.0 and 1.8. The same breast specimens were then imaged with the PLS 5C1 synchrotron imaging system using the following image acquisition parameters: an exposure time of 800 msec and a silicon wafer filter with a thickness of 1.0 mm at an object-to-scintillator distance of approximately 300 mm. In this study, all of the images acquired with the conventional mammographic system were scanned and digitized with a commercial scanner (Epson Perfection 1200S; Nagano, Japan), and all of the images acquired with the synchrotron radiation imaging system were inverted, in order to compare them with the conventional mammography images. The final images, which exceeded the field-of-view of the CCD camera, were obtained by patching together multiple small images.

RESULTS

The PLS 5C1 imaging system showed a spatial resolution of at least 20 line-pairs mm-1 (25μm) with the image of the resolution test pattern (Nuclear Associates Co., Hicksville, NY, USA). Fig. 3 shows a comparison of the resolution ob-

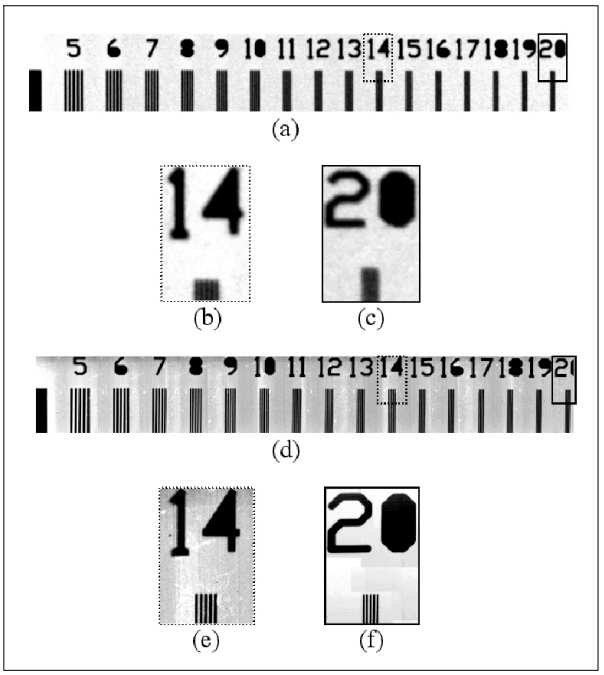

Fig. 3. The images of the spatial resolution test pattern; (a) complete image, (b) small input field of 14 line pairs mm^{-1}, and (C) small input field of 20 line pairs mm^{-1}, obtained by the conventional mammography system (GE Senographe DMR) and (d) complete image, (e) small input field of 14 line pairs mm^{-1}, and (f) small input field of 20 line pairs mm^{-1}, obtained by the PLS 5C1 synchrotron imaging system. The PLS 5C1 unmonochromatized synchrotron imaging system provided a resolution of at least 20 line-pairs mm^{-1} (25 μm) with the resolution test pattern compared to the 14 line-pairs mm^{-1} ($\approx$36 μm) spatial resolution obtained with the conventional mammography system.

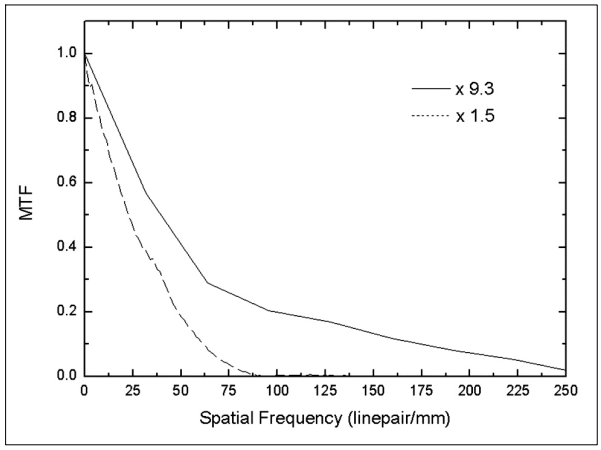

Fig. 4. The modulation transfer function (MTF) of the PLS 5C1 SR imaging system at 1.5 × and 9.5 × optical magnifications for the horizontal direction in relation to the incident beam. The spatial resolution (10% of MTF) was found to be about 60 line pairs/mm (corresponds to 8.3 nm) for the imaging setup with 1.5 × optical magnification.

tained with the PLS 5C1 imaging system with that obtained with the conventional mammography system. The results of the MTF measurements showed that the spatial resolution was improved by the magnified imaging of the object. For the imaging setup with the 1.5 × optical magnification, the vertical spatial resolution was found to be 8.3 nm, which corresponds to about 60 line pairs/mm (Fig. 4). The limiting spatial resolution, which is the maximum resolution of an imaging system achievable under optimal conditions, was about 3.1 mm, which is the same as the equivalent image pixel size for 1.5 × magnification.

Fig. 5 shows the images of the glass capillary tube filled with air bubbles demonstrating the coherence-based edge enhancement. An Intensity profile was taken along the vertical line, obtaining the result shown in Fig. 5(f), in which the cross-sectional intensity profile of the bubble produced by the coherence-based edge enhancement can be seen.

The mammographic phantom images (Gammex RMI 156) obtained with the synchrotron X-ray system were not able to be evaluated according to the American College of Radiology (ACR) criteria, since the size of the imaging field of view for this system was too small to image the full size of the mammographic phantom. Hence, specific regions

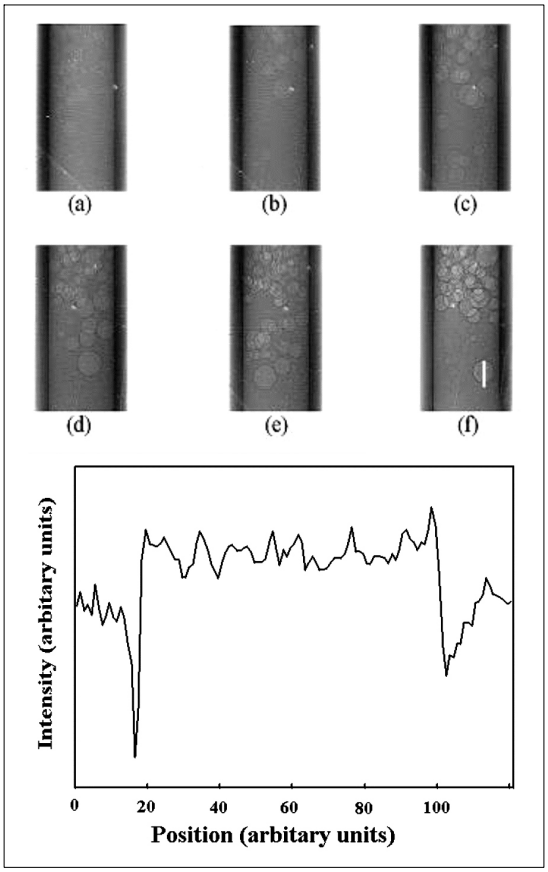

Fig. 5. The PLS 5C1 unmonochromatized synchrotron radiation images of a glass capillary tube filled with air bubbles for various object-to-detector (scintillator) distances viz. for (a) to (f), 50, 100, 200, 250, 300, and 470 mm, respectively. The sequential images illustrate the effect of the coherence-based contrast which operates by the mechanism of refraction-based edge enhancement within a certain range of object-detector distance values. (g) Cross-sectional intensity profile of the bubble along the vertical line in (f) (arbitrary units scaled to each other).

of the microcalcifications imaged with the synchrotron X-ray system were compared with the images of the same regions obtained by conventional mammography and the former showed much greater detail in the simulated region within the mammographic phantom (Fig. 6).

Fig. 7 shows the photographic and radiological images of one human breast specimen selected from among the ten human breast specimens. The images obtained form the formalin fixed human breast tissue with the synchrotron X-ray system showed much higher spatial resolution with better image contrast. Greater details and clearer bound-

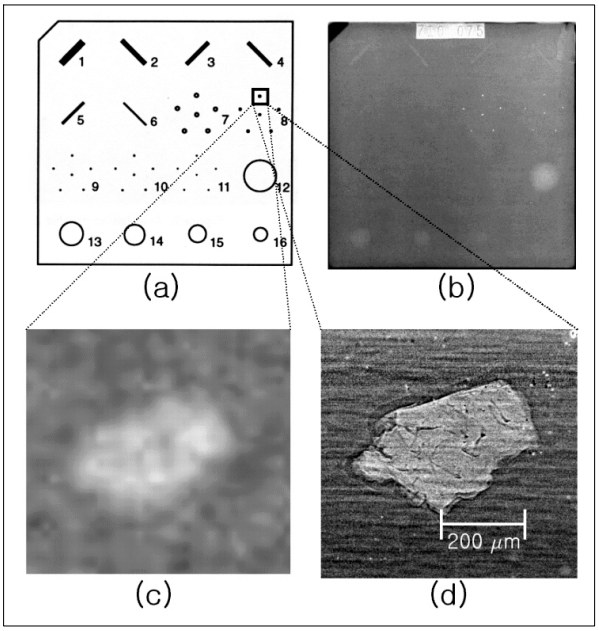

Fig. 6. Schematic and images of the mammographic accreditation phantom (Gammex RMI 156); (a) a schematic view of the mammographic phantom giving the test object sizes and positions, (b) radiographic image obtained with the conventional mammographic system, (c) partial image of artificial microcalcification obtained with the conventional mammography system, (d) partial image of artificial microcalcification obtained with the PLS 5C1 synchrotron imaging system. The synchrotron image of artificial microcalcification shows more details and clearer boundaries.

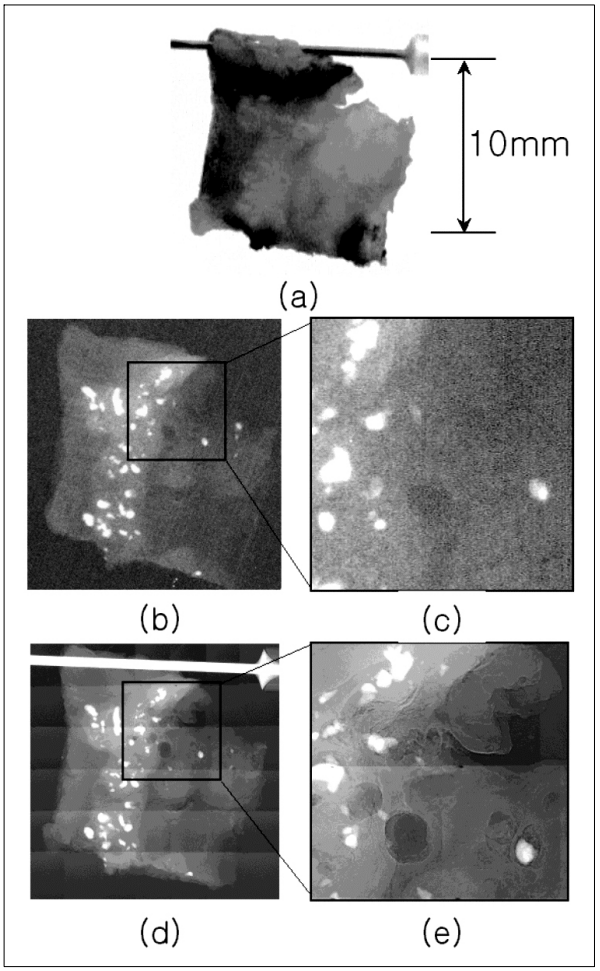

Fig. 7. Images of human breast cancer specimens preserved in formalin acquired from conventional mammographic system and the PLS 5C1 unmonochromatized synchrotron imaging system; (a) gross photographic image of specimen, (b) whole image, and (c) small input field of image b obtained with the conventional mammography system, (d) complete image, and (e) small input field of image obtained with the synchrotron radiation imaging system. In the images (b)-(e), white spots show the images of the microcalcifications detected in the breast cancer tissue. In the synchrotron radiation images, the contrast was enhanced and the details were depicted more sharply than in the conventional images. In particular, the edges of the calcification and mass were well defined. Here, the synchrotron radiation images were inverted for the purpose of comparison with the mammographic images. (In the synchrotron radiation images, the upper and right white bars indicate the needle used for hanging the specimen during image acquisition.)

aries inside of the tissues can clearly be seen in these images. The magnified synchrotron X-ray image in Fig. 7 shows not only the number of microcalcifications, but also the finer details of their shapes, which may be of high clinical significance in the examination of breast tissues. In general, the images obtained from the 5C1 SR imaging system showed details, which would not to be able to be visualized using other imaging modalities.

DISCUSSION

Conventional X-rays have been widely used in medical applications such as diagnostic imaging. Typically, braking radiation and characteristic X-rays were used, with the contrast being based on the absorption characteristics. In contrast, synchrotron X-rays can produce a superior image quality, which is characterized by high resolution and coherence-based edge enhancement, and which is aided by the high beam collimation and coherence. This coherence-based contrast requires

a high level of lateral coherence, but not longitudinal coherence, as demonstrated in our previous report.[8] The blur on the refraction-enhanced images is very limited, due to the fact that the real part of the refraction index is very sensitive to the wavelength, in the wavelength range of the photons used in this study. The high intensity, tunable energy and polarization of the synchrotron radiation make it an ideal X-ray source for many applications in the medical sciences.

Several research groups have investigated these coherence-based contrast techniques using monochromatized synchrotron radiation in biological soft tissue and tried to utilize these methods for clinical applications, such as mammography.[18,19] Coherence-based contrast techniques enhance the image quality, and are especially effective at the borders of thin biological soft tissues, however, there is no strict requirement for either monochromatized or coherent radiation to be used.[4,8] Our research group has recently extended coherence-based contrast imaging to unmonochromatized synchrotron X-rays with a simple imaging system.

The images of the air bubbles in Fig. 5 are examples intended to demonstrate that the coherence-based edge enhancement depends on the test object-to-detector distances, which is an essential feature of coherence-based radiography. In particular, the fringe-like enhancements found on the boundaries of the bubbles and the glass capillary tube walls are notable. This effect is due to the refraction of the X-ray beam when it enters areas of different refractive index. Using this concept, we successfully demonstrated the capability of the system to achieve micrometer resolution in this study.

The spatial resolution of the PLS 5C1 imaging system was at least 20 line-pairs mm^{-1} (25μm) with the resolution test pattern used in this study. A higher resolution test pattern or the quantitative evaluation method may be needed to further evaluate the resolution limitation of the PLS 5C1 synchrotron imaging system. The images of the human breast tissues obtained with the synchrotron X-rays showed much higher spatial resolution with better image contrast and provided greater details and clearer boundaries inside of the tissues than those obtained with conventional mammography. Fine internal structures of the human breast tissue specimens were visualized with resolutions of a few micrometers and enhanced edge contrast. However, there may be a greater possibility of image blurring caused by Compton scattering for thicker biological samples when using the unmonochromatic synchrotron radiation than when using the monochromatic synchrotron radiation. The magnified synchrotron X-ray image in Fig. 7 shows not only the number of microcalcifications but also their shapes, which may have clinical significance for the analysis of the early stage of breast cancers. The 5C1 synchrotron radiation imaging system provided micrometer resolution images with fine/numerous details of the tissue structures, which may not be able to be visualized by other imaging modalities.

The radiation doses delivered in monochromatic SR mammography when using a mammographic phantom were reported to be almost the same as those delivered with the conventional grid technique.[20] The radiation dose may constitute a real limitation to the use unmonochromatized SR imaging system in clinical applications. The specific radiation dose problem exists in our approach at the current version, although it may be able to be improved with the automatic fast shuttering system, which is slated to be developed in the near future. Meanwhile, it should be noted that the radiation dose will inevitably be increased when ultra high-resolution is required with higher magnification.

The high quality images obtained in this work also confirm that coherence-based contrast imaging can be realized without sophisticated experimental facilities, while demonstrating that our approach can provide the same level of image quality as the other approaches.

Although further research studies are required to utilize these techniques, including the one proposed herein, in clinical applications, we believe that the simplicity of our approach could be beneficial in the application of unmonochromatized synchrotron radiation to medical imaging.

REFERENCES

1. Momose A, Fukuda J. Phase-contrast radiographs of nonstained rat cerebellar specimen. Med Phys 1995;

22:375-9.
2. Davis TJ, Gao D, Gureyev TE, Stevenson AW, Wilkins SW. Phase-contrast imaging of weakly absorbing materials using hard x-rays. Nature 1995;373:595-8.
3. Snigirev A, Snigireva I, Kohn V, Kuznetsov S, Schelokov I. On the possibilities of x-ray phase contrast microimaging by coherent high-energy synchrotron radiation. Rev Sci Instrum 1995;66:5486-92.
4. Wilkins SW, Gureyev TE, Gao D, Pogany A, Stevension AW. Phase-contrast imaging using polychromatic hard x-rays. Nature 1996;384:335-8.
5. Chapman D, Thomlinson W, Johnston RE, Washburn D, Pisano ED, Gmur NF, et al. Diffraction enhanced x-ray imaging. Phys Med Biol 1997;42:2015-25.
6. Gao D, Pogany A, Stevenson AW, Wilkins SW. Phase-contrast radiography. Radiographics 1998;18:1257-67.
7. Margaritondo G, Tromba G. Coherence-based edge diffraction sharpening of x-ray images: a simple model. J Appl Phys 1999;85:3406-8.
8. Hwu Y, Hsieh HH, Lu MJ, Tsai WL, Lin HM, Goh WC, et al. Coherence-enhanced synchrotron radiation: refraction versus diffraction mechanisms. J Appl Phys 1999;86;4613-8.
9. Kim HJ, Hong JO, Lee KH, Jung H, Kim EK, Je JH, et al. Phantom and animal imaging studies using PLS synchrotron x-rays. IEEE T Nucl Sci 2001;48:837-42.
10. Hwu Y, Je JH, Lee KH, Margaritondo G. Real time micro-radiology with SR on live specimens. 7th International Conference on Synchrotron Radiation Instrumentation, Book of Abstracts, THU2-01 invited 2000.
11. Hwu Y, Tsai WL, Hsieh HH, Je JH, Kang HS, Kim IW, et al. Collimation-enhanced micro-radiography in real-time. Nucl Instrum Meth A 2001;467-8:294-1300.
12. Yoneyama A, Momose A, Seya E, Hirano K, Takeda T, Itai Y. Operation of a separated-type x-ray interferometer for phase-contrast x-ray imaging. Rev Sci Instrum 1999;70:4582-6.
13. Takeda T, Momose A, Hirano K, Haraoka S, Watanabe T, Itai Y. Human carcinoma: early experience with phase-contrast x-ray CT with synchrotron radiation-comparative specimen study with optical microscopy. Radiology 2000;214:298-301.
14. Pisano ED, Johnston RE, Chapman D, Geradts J, Lacocca MV, Livasy CA, et al. Human breast cancer specimens: diffraction-enhanced imaging with histologic correlation-improved conspicuity of lesion detail compared with digital radiography. Radiology 2000; 214:895-901.
15. Jung H, Kim HJ, Hong S, Hong JO, Jeong HK, Je JH, et al. Computed microtomography (μCT) with unmonochromatized synchrotron X-rays for cancerous human breast tissue and mouse vertebra. IEEE T Nucl Sci 2002;49:2262-7.
16. Hwu Y, Lai B, Mancini DC, Je JH, Noh DY, Bertolo M, et al. Coherence based contrast enhancement in x-ray radiography with a photoelectric microscope. Appl Phys Lett 1999;75:2377-9.
17. Umetani K, Yagi N, Suzuki Y, Kohmura Y, Yamasaki K. X-ray refraction-contrast imaging using synchrotron radiation at Spring-8. Medical Imaging 1999 Physics of Medical Imaging. Proceedings of SPIE 1999;3659:560-71.
18. Yu Q, Takeda T, Umetani K, Ueno E, Itai Y, Hiranaka Y, et al. First experiment by two-dimensional digital mammography with synchrotron radiation. J Synchrotron Rad 1999;6:1148-52.
19. Arfelli F, Bonvicini V, Bravin A, Cantatore G, Castelli E, Palma LD, et al. Mammography with synchrotron radiation: phase-detection techniques. Radiology 2000; 215:286-93.
20. Burattini E, Cossu E, Maggio CD, Gambaccini M, Indovina PL, Marziani M, et al. Mammography with synchrotron radiation. Radiology 1995;195:239-44.